



THE UNIVERSITY *of* EDINBURGH

## Edinburgh Research Explorer

### Effects of ultrasound on electrochemical oxidation mechanisms of p-substituted phenols at BDD and PbO<sub>2</sub> anodes

**Citation for published version:**

Zhu, X, Ni, J, Li, H, Jiang, Y, Xing, X & Borthwick, AGL 2010, 'Effects of ultrasound on electrochemical oxidation mechanisms of p-substituted phenols at BDD and PbO<sub>2</sub> anodes', *Electrochimica Acta*, vol. 55, no. 20, pp. 5569-5575. <https://doi.org/10.1016/j.electacta.2010.04.072>

**Digital Object Identifier (DOI):**

[10.1016/j.electacta.2010.04.072](https://doi.org/10.1016/j.electacta.2010.04.072)

**Link:**

[Link to publication record in Edinburgh Research Explorer](#)

**Published In:**

Electrochimica Acta

**General rights**

Copyright for the publications made accessible via the Edinburgh Research Explorer is retained by the author(s) and / or other copyright owners and it is a condition of accessing these publications that users recognise and abide by the legal requirements associated with these rights.

**Take down policy**

The University of Edinburgh has made every reasonable effort to ensure that Edinburgh Research Explorer content complies with UK legislation. If you believe that the public display of this file breaches copyright please contact [openaccess@ed.ac.uk](mailto:openaccess@ed.ac.uk) providing details, and we will remove access to the work immediately and investigate your claim.



# Effects of Ultrasound on Electrochemical Oxidation of *p*-Substituted Phenols at BDD and PbO<sub>2</sub> Anodes

## Abstract

The effects of ultrasound are investigated with regard to the effectiveness and mechanisms of electrochemical oxidation of *p*-substituted phenols (*p*-nitrophenol, *p*-hydroxybenzaldehyde, phenol, *p*-cresol, and *p*-methoxyphenol) at BDD (boron-doped diamond) and PbO<sub>2</sub> anodes. Although ultrasound substantially improved the degradation rates of *p*-substituted phenols at both the BDD and PbO<sub>2</sub> anodes, the degree of enhancement varied according to the type of *p*-substituted phenol and type of anode under consideration. A parameter called the %Synergy is defined as the percentage ratio of the difference between first-order rate constants evaluated without and with ultrasound to the first-order rate constant without ultrasound. The %Synergy parameter gives an indirect measure of the synergy between the ultrasound and the electrochemical oxidation process. At the BDD anode, the %Synergy values were in the range 73-83% for *p*-substituted phenol degradation and in the range 60~70% for COD removal. However, at the PbO<sub>2</sub> anode, the corresponding %Synergy values were in the range 50~70% for degradation of *p*-substituted phenols and only 5~25% for COD removal, much lower values that obtained at the BDD anode. Further investigations on the influence of ultrasound on the electrochemical oxidation mechanisms at BDD and PbO<sub>2</sub> anodes revealed that the different synergies were due to the specialized electrochemical oxidation mechanisms at these two anodes. The hydroxyl radicals were mainly free at the BDD electrodes, but absorbed at the PbO<sub>2</sub> electrodes. Ultrasound was more beneficial to the indirect electrochemical oxidation mediated by free hydroxyl radicals because absorbed hydroxyl radicals readily combined to form oxygen in the presence of ultrasound. Therefore, the enhancement due to ultrasound was greater at the BDD anode

1 than at the  $\text{PbO}_2$  anode.

2

## 1 Introduction

2 Phenols are typical organic pollutants. They are toxic and bio-refractory. Many industrial  
3 processes generate effluents containing phenol compounds; for example, the production of pesticides,  
4 herbicides, dyes, textiles, pharmaceuticals, pulp, paper, plastics, and detergents (1-3). Conventional  
5 biological methods have not proven very effective at treating industrial wastewaters containing  
6 phenol compounds. Electrochemical oxidation offers a promising technological solution to the  
7 treatment of bio-refractory wastewaters, because it is environmentally clean, efficient at organic  
8 degradation, easy to control, and simple in structure (4).

9 Anode materials play an important part in electrochemical oxidation technology. Different  
10 anode materials lead to different electrochemical oxidation mechanisms, effectiveness and  
11 efficiencies. In general, at active anodes, such as Pt, IrO<sub>2</sub>, and RuO<sub>2</sub>, the hydroxyl radicals produced  
12 by water decomposition interact with the oxide anode and are transferred to the lattice of the oxide  
13 anode to form chemisorbed "active oxygen" (oxygen in the oxide lattice, MO<sub>x+1</sub>). This oxidant  
14 MO<sub>x+1</sub> has weak oxidation ability, and thus the active anodes have low reactivity regarding organic  
15 oxidation (5-7). Although hydroxyl radicals do not react with non-active anodes, such as PbO<sub>2</sub>, SnO<sub>2</sub>,  
16 and BDD (boron-doped diamond), the organic compounds instead react with hydroxyl radicals (·OH)  
17 at non-active anodes. Because the hydroxyl radical is a strong oxidant, the PbO<sub>2</sub>, SnO<sub>2</sub>, and BDD  
18 anodes exhibit high oxidation capability for degrading organic pollutants (8-14). However, compared  
19 to PbO<sub>2</sub> and SnO<sub>2</sub> anodes, BDD electrodes appear to have much higher oxidation ability (9-12).  
20 Recent studies (3, 15) demonstrate that the enhanced oxidation may be due to the existence of  
21 different types of hydroxyl radicals at PbO<sub>2</sub>, SnO<sub>2</sub>, and BDD electrodes. At BDD anodes, the  
22 hydroxyl radicals mainly exist as free hydroxyl radicals, which react effectively with organic  
23 pollutants. At PbO<sub>2</sub> anodes, absorbed hydroxyl radicals dominate, and are not very effective for the  
24 oxidation of organic compounds. At SnO<sub>2</sub> anodes, the organic compounds reacted with both

1 adsorbed hydroxyl radicals and free hydroxyl radicals.

2 Under normal operating conditions, electrochemical oxidation processes are under  
3 mass-transport control (16, 17). As a result, the enhancement of mass transport would appear to be a  
4 very important factor in optimizing the electrochemical oxidation processes. Many studies (18-21)  
5 have proved that ultrasound can significantly improve mass transfer. It therefore seems reasonable  
6 that the combination of electrochemical oxidation and ultrasound could be particularly useful.  
7 Several studies (22-24) have demonstrated that enhanced electrochemical oxidation of phenol and 2,  
8 4-dihydroxybenzoic acid at Pt and BDD electrodes can be attributed to improved mass transfer due  
9 to the effect of ultrasound. However, to the authors' knowledge no published studies have  
10 investigated the influence of ultrasound on electrochemical oxidation mechanisms. There is  
11 presently confusion as to which reactions are enhanced and which are weakened by the presence of  
12 ultrasound during electrochemical oxidation.

13 The present study investigates the effect of ultrasound on electrochemical oxidation  
14 mechanisms at BDD and PbO<sub>2</sub> anodes, with the aim of gaining a better understanding of the reaction  
15 mechanisms. BDD and PbO<sub>2</sub> electrodes were chosen because they have strong oxidation  
16 characteristics, have been the subject of much research (see e.g. Reference), and promote  
17 fundamentally different types of hydroxyl radicals at their surface.

## 19 **Experimental Procedures**

### 20 **Bulk electrolysis**

21 Electrochemical oxidation of *p*-substituted phenols (*p*-nitrophenol, *p*-hydroxybenzaldehyde,  
22 phenol, *p*-cresol, and *p*-methoxyphenol) was performed at constant current density (20 mA cm<sup>-2</sup>) and  
23 room temperature (25 °C). The volume of electrolyte was 250 mL. In the absence of ultrasound, the  
24 electrolyte was stirred by a magnetic stirring bar during the electrolysis process. In the presence of

ultrasound, the cell was put into an ultrasound rinse slot (40 kHz, 150 W). To keep the room temperature constant, tap water continuously flowed through the rinse slot. The anode comprised either a BDD or a PbO<sub>2</sub> electrode, with an exposed geometric area of 4 cm<sup>2</sup>. A stainless steel sheet of the same size was used as the cathode. The electrode gap was 10 mm. Samples were collected from the cell at prescribed intervals for chemical analysis.

The concentration of *p*-substituted phenols was measured using Agilent HP1100 HPLC with a ZORBAX SB-C18 column and a DAD detector. The mobile phase was methanol/water (50/50) with a flow rate of 1.0 mL min<sup>-1</sup>. The UV detector was set at 314 nm for *p*-nitrophenol, and 280 nm for other *p*-substituted phenols. Chemical oxygen demand (COD) was measured by a titrimetric method using dichromate as the oxidant in acidic solution at 150 °C for two hours (Hachi, USA).

### Electrochemical measurement

The electrochemical measurements were performed using a CHI 760B electrochemical workstation (Shanghai Chenhua, China). The working electrode was the BDD or PbO<sub>2</sub> electrode. A platinum plate was used as the auxiliary electrode, while a saturated calomel electrode (SCE) was used as the reference electrode in a separate compartment connected to the reactor by a salt bridge (all potentials are quoted against SCE).

### Detection of electrogenerated oxidants

I<sup>-</sup>/I<sub>2</sub> assays were performed to measure electrogenerated oxidants (1, 15). Electrolysis was carried out in 250 mL Na<sub>2</sub>SO<sub>4</sub> solution. Every 0.5h, a 5 mL sample was collected from the electrolysis cell. 10 mL 0.01 M KI and 5 mL HCl (1:1) were then immediately added to the sample, which was then stored in the dark for 5 min. Finally, 1 mM Na<sub>2</sub>S<sub>2</sub>O<sub>3</sub> was used to titrate the amount of produced I<sub>2</sub> in the presence of starch. The concentration of electrogenerated oxidants (*C*<sub>EO</sub>) was calculated using following equation:

$$C_{eo} = V C / (4 V_s) \quad (\text{mM O}_2) \quad (1)$$

where  $V$  is the volume of  $\text{Na}_2\text{S}_2\text{O}_3$  solution used for titration (in mL),  $C$  is the concentration of  $\text{Na}_2\text{S}_2\text{O}_3$  solution (in mM),  $V_s$  is the volume of collected sample (in mL), and 4 is a factor for charge conservation ( $1 \text{ mol O}_2 \text{ mol}^{-1} e^{-1} / 4 \text{ mol S}_2\text{O}_3^{2-} \text{ mol}^{-1} e^{-1}$ ).

$$C_{EO}(\text{mM O}_2) = \frac{V_{\text{S}_2\text{O}_3^{2-}} C_{\text{S}_2\text{O}_3^{2-}}}{4V_{\text{sample}}} \quad (1)$$

where  $V_{\text{S}_2\text{O}_3^{2-}}$  is the volume of  $\text{Na}_2\text{S}_2\text{O}_3$  solution used for titration (in mL),  $C_{\text{S}_2\text{O}_3^{2-}}$  is the concentration of  $\text{Na}_2\text{S}_2\text{O}_3$  solution (in mM),  $V_{\text{sample}}$  is the volume of collected sample (in mL), and 4 is a factor for charge conservation ( $1 \text{ mol O}_2 \text{ mol}^{-1} e^{-1} / 4 \text{ mol S}_2\text{O}_3^{2-} \text{ mol}^{-1} e^{-1}$ ).

### Detection of hydroxyl radicals

According to references (8, 15), N, N-dimethy-p-nitrosoaniline (RNO) was used for spin trapping the hydroxyl radicals. Electrolysis was performed in a 250 mL phosphate buffer (pH=7.1) solution containing 20  $\mu\text{M}$  RNO. The bleaching of the yellow color (RNO) during electrolysis process was measured at 440 nm using UV-Visible spectrophotometer (Specord 200, Analytikjena).

### Mass Transfer Measurement

The mass transfer coefficient was obtained by electrochemical measurement (18, 22, 25). The electrochemical system comprised a ferro/ferricyanide redox couple ( $5 \text{ mmol l}^{-1} \text{ K}_2[\text{Fe}^{\text{II}}(\text{CN})_6]$  and  $5 \text{ mmol l}^{-1} \text{ K}_3[\text{Fe}^{\text{III}}(\text{CN})_6]$ ) in alkaline media ( $\text{NaOH } 0.5 \text{ mol l}^{-1}$ ). When the potential of the working electrode was controlled at -0.1 V vs. SCE, in the plateau zone of the ferricyanide reduction, the resulting reduction current was diffusion controlled and related to:

$$i_L = n F S D_{\text{OX}} \frac{C_{\text{OX,S}}}{\delta} \quad (2)$$

where  $i_L$  the diffusion current (in A),  $n$  the number of exchanged electrons per anion ( $n=1$ ),  $F$  the Faraday constant ( $96487 \text{ C mol}^{-1}$ ),  $S$  the electrode surface area ( $4 \times 10^{-4} \text{ m}^2$ ),  $D_{\text{OX}}$  the diffusion coefficient of ferricyanide ( $0.9 \times 10^{-9} \text{ m}^2 \text{ s}^{-1}$ ),  $C_{\text{OX,S}}$  the bulk solution concentration of ferricyanide ( $5$

1 mol m<sup>-3</sup>), and  $\delta$  the double layer thickness (in m).

2 Then, the mass transfer coefficient is calculated by:

3 
$$k_d = \frac{D_{ox}}{\delta} = \frac{i_L}{nFSC_{ox, s}} \quad (3)$$

## 4 **Results and Discussion**

### 5 **Bulk electrolysis in the absence and presence of ultrasound**

6 Electrochemical oxidation of *p*-substituted phenols (*p*-nitrophenol, *p*-hydroxybenzaldehyde,  
7 phenol, *p*-cresol, and *p*-methoxyphenol) at the BDD and PbO<sub>2</sub> anodes was performed in the absence  
8 and presence of ultrasound, respectively. Figure 1 shows the evolution of substrate concentration and  
9 COD during the bulk electrolysis. It can be observed that the degradation rates of the substrates and  
10 COD were both improved by ultrasound. However, the enhancements varied according to the  
11 particular choice of *p*-substituted phenol and specialized anode. Table 1 lists the rate constants of  
12 *p*-substituted phenol and COD degradation at the BDD and PbO<sub>2</sub> anodes in the absence ( $k_{ele}$ ) and  
13 presence ( $k_{sonel}$ ) of ultrasound, obtained by fitting the concentration data to the following pseudo-first  
14 order kinetic equation (eq 4) (14, 26, 27),

15 
$$C(t) = C_0 \exp(-kt) \quad (4)$$

16 where  $C(t)$  is the concentration at time  $t$  (in h),  $C_0$  is the initial concentration, and  $k$  is the rate  
17 constant (in h<sup>-1</sup>).

18 In the present study, the low-frequency ultrasound did not itself degrade the *p*-substituted  
19 phenols; instead the degradation resulted from a synergetic process involving both ultrasound and  
20 electrochemical oxidation. We estimated this synergy using the following equation:

21 
$$\% \text{ Synergy} = \frac{(k_{sonel} - k_{elec})}{k_{sonel}} 100 \quad (5)$$

22 Figure 2 is a histogram showing the %Synergy levels obtained for the five *p*-substituted phenols  
23 in terms of phenol degradation and COD degradation at the BDD and PbO<sub>2</sub> anodes. At the BDD



anode, the values of %Synergy were in the range 73~83% for *p*-substituted phenols degradation and 60~70% for COD removal. Compared to the BDD electrode, the values of %Synergy obtained for the PbO<sub>2</sub> anode were much lower: 50~70% for phenol degradation and only 5~25% for COD removal. The %Synergy values for COD removal were lower than those for phenol degradation at both the BDD and PbO<sub>2</sub> anodes, due to the formation of intermediate chemicals (27-29). The differences in %Synergy values obtained for the same *p*-substituted phenols at the BDD and PbO<sub>2</sub> anodes are due to the different electrochemical oxidation mechanisms at these two anodes. In the next section, we carry out a thorough investigation into the effects of ultrasound on the electrochemical oxidation mechanisms at BDD and PbO<sub>2</sub> anodes.

### Effects of ultrasound on electrochemical oxidation mechanisms

The electrochemical oxidation mechanisms could be (1, 15): (1) direct electrochemical oxidation on the BDD and PbO<sub>2</sub> surfaces, (2) indirect electrochemical oxidation mediated by electrogenerated oxidants at BDD anodes, such as peroxodisulfates (in the presence of SO<sub>4</sub><sup>2-</sup>) and active chlorine (in the presence of Cl<sup>-</sup>), and (3) indirect electrochemical oxidation mediated by free hydroxyl radicals at BDD anodes and absorbed hydroxyl radicals at PbO<sub>2</sub> anodes.

Electrochemical measurements were performed to investigate the direct electrochemical oxidation. Figure 3 shows the cyclic voltammograms of the five *p*-substituted phenols at the BDD and PbO<sub>2</sub> electrodes, in the absence and presence of ultrasound. For the BDD electrode, the oxidation current of all *p*-substituted phenols substantially increased in the presence of ultrasound, indicating that the direct electrochemical oxidation of the *p*-substituted phenols would be greatly improved by ultrasound. However, the ascending order of the phenols with regard to oxidation peak current (Ph-OCH<sub>3</sub> ≈ Ph-CH<sub>3</sub> > Ph-OH > Ph-CHO > Ph-NO<sub>2</sub>) was opposite to their ascending order in terms of degradation rate (Ph-NO<sub>2</sub> > Ph-CHO ≈ Ph-OH > Ph-CH<sub>3</sub> > Ph-OCH<sub>3</sub>) during bulk electrolysis in

1 the presence of ultrasound. Hence, enhancement of the phenol degradation rates during bulk  
2 electrolysis was not due to improvement of direct electrochemical oxidation by ultrasound. This was  
3 most likely because direct electrochemical oxidation was not the main reaction during electrolysis  
4 processes, as also observed in previous studies (3, 15). Moreover, the oxidation peak current in the  
5 second cycle decreased more quickly in the presence than in the absence of ultrasound, which meant  
6 that electrode fouling would be accelerated in the presence of ultrasound when direct  
7 electrochemical oxidation occurred. For the PbO<sub>2</sub> electrode, the oxidation peak current and hence  
8 electrochemical oxidations of *p*-substituted phenols were only slightly enhanced in the presence of  
9 ultrasound. This implies that the raised phenol degradation rates during bulk electrolysis at the PbO<sub>2</sub>  
10 anode are not due to the increased direct electrochemical oxidation by ultrasound.

11 In the presence of sulfates (SO<sub>4</sub><sup>2-</sup>), peroxodisulfates (S<sub>2</sub>O<sub>8</sub><sup>2-</sup>) form, of which a proportion  
12 decomposes to hydrogen peroxide and other oxidants at BDD anodes (1, 28). In the present  
13 investigation, I<sup>-</sup>/I<sub>2</sub> assays were performed to measure the electrogenerated oxidants. Figure 4 shows  
14 the evolution of electrogenerated oxidant concentration at the BDD anode in the absence and  
15 presence of ultrasound. Surprisingly, the electrogenerated oxidant concentration in the presence of  
16 ultrasound was lower than that in the absence of ultrasound, which might be due to the lower  
17 stability of electrogenerated oxidants in the presence of ultrasound. This result indicates that  
18 enhancement of the phenol degradation rates during bulk electrolysis at the BDD anode was not due  
19 to better indirect electrochemical oxidation mediated by electrogenerated oxidants. It also confirmed  
20 that indirect electrochemical oxidation mediated by electrogenerated oxidant was not the main  
21 reaction at the BDD anodes, consistent with the previous study (15).

22 Therefore, it can be deduced that indirect electrochemical oxidation mediated by hydroxyl  
23 radicals was the main reaction at BDD and PbO<sub>2</sub> anodes, and the improvement of *p*-substituted  
24 phenol degradation could be mainly attributed to enhancement of this mechanism by ultrasound.

1 Figure 5 plots the time-evolution of the hydroxyl radical concentrations at the BDD and PbO<sub>2</sub>  
 2 anodes in the absence and presence of ultrasound. In all cases, the hydroxyl radical concentrations  
 3 increased and appear to be tending to saturate at a value close to  $20 \times 10^{-6}$  M. The presence or  
 4 otherwise of ultrasound seems to have little effect on the hydroxyl radical concentration curve with  
 5 time for the PbO<sub>2</sub> anode. But, the presence of ultrasound increased mass transfer at the BDD node,  
 6 thus substantially raising the rate of increase of the hydroxyl radical concentration curve. By  
 7 electrochemical measurement, the mass transfer coefficients were estimated as follows:  $2.00 \times 10^{-5}$   
 8  $\text{m s}^{-1}$  without ultrasound and  $4.99 \times 10^{-5} \text{ m s}^{-1}$  with ultrasound at the BDD anode; and  $1.02 \times 10^{-4} \text{ m}$   
 9  $\text{s}^{-1}$  without ultrasound and  $1.31 \times 10^{-4} \text{ m s}^{-1}$  with ultrasound at the PbO<sub>2</sub> anode. The increased mass  
 10 transfer coefficients at the PbO<sub>2</sub> electrode relative to those at the BDD electrode can be attributed to  
 11 the stronger absorption capacity of PbO<sub>2</sub> electrodes. For both types of anode, the increase of mass  
 12 transfer coefficients was similar ( $\sim 2.9 \times 10^{-5} \text{ m s}^{-1}$ ) in the presence of ultrasound, indicating that the  
 13 influence of ultrasound on mass transfer was the same. Hence, the different increases in hydroxyl  
 14 radical concentration obtained at the BDD and PbO<sub>2</sub> anodes in the presence of ultrasound may be  
 15 attributed to the affect of fundamentally different types of hydroxyl radicals. At BDD electrodes, the  
 16 hydroxyl radicals mainly exist as free hydroxyl radicals due to their weak adsorption properties (9,  
 17 11, 15, 30). Such hydroxyl radicals do not readily combine with each other to produce oxygen (as a  
 18 side reaction) in the presence of ultrasound and have strong oxidation ability. Hence, ultrasound led  
 19 to a higher rate of increase of hydroxyl radical concentration and hence more rapid degradation of  
 20 phenol compounds at the BDD anode than at the PbO<sub>2</sub> node. Instead, the hydroxyl radicals at PbO<sub>2</sub>  
 21 electrodes exist in an adsorbed state and so such electrodes have strong adsorption properties (9, 11,  
 22 15, 30). Such hydroxyl radicals combine easily to form oxygen in the presence of ultrasound, leading  
 23 to a relatively weaker oxidation capacity. Thus, the increase of hydroxyl radical concentration at the  
 24 PbO<sub>2</sub> anode was lower and the enhancement of *p*-substituted phenols oxidation was not so obvious

1 in the presence of ultrasound.

2 The above finding was further confirmed by the increasing linear relationship observed between  
3 the rate constant ( $k$ ) of  $p$ -substituted phenols and Hammett's constant ( $\sigma$ ) at the BDD electrode  
4 (Figure 6A), and between the rate constant ( $k$ ) of  $p$ -substituted phenols and the initial surface  
5 concentration ( $\Gamma$ ) at the  $\text{PbO}_2$  anode (Figure 6B). Hammett's constant represents the effect of  
6 different substituents on the electron character of a given aromatic system. A positive value of  
7 Hammett's constant indicates an electron-withdrawing group, while a negative value indicates an  
8 electron-donating group. The initial surface concentration indicates the capacity of phenols to be  
9 adsorbed to the electrode surface (see (15) for more details).

10 At the BDD electrodes, the hydroxyl radicals mainly exist as free hydroxyl radicals, which  
11 directly attack the substrates, first removing  $p$ -substituted groups from the aromatic ring. Since  
12 electron-withdrawing groups are easily released,  $p$ -substituted phenols within these groups are  
13 degraded faster than those within electron-donating groups. Therefore, the degradation rate of  
14  $p$ -substituted phenols increases monotonically with Hammett's constant. In the presence of  
15 ultrasound, the already enhanced phenol degradation rate was further increased with increasing  
16 Hammett's constant. This implies that indirect electrochemical oxidation mediated by free  
17 hydroxyl radicals was significantly improved by ultrasound at the BDD anode.

18 On the other hand, at the  $\text{PbO}_2$  anode, hydroxyl radicals mainly existed as adsorbed hydroxyl  
19 radicals, and these adsorbed hydroxyl radicals reacted with substrates on the anode surface. Hence,  
20 the degradation rate of  $p$ -substituted phenols increased with the increase of initial surface  
21 concentration rather than with Hammett's constant. The degradation rates of  $p$ -substituted phenols  
22 were improved both by the presence of ultrasound and by raised initial surface concentration, thus  
23 demonstrating that indirect electrochemical oxidation mediated by adsorbed hydroxyl radicals was  
24 improved by ultrasound at the  $\text{PbO}_2$  anode.

Figure 6 also shows that the increase in *p*-substituted phenols degradation at the BDD anode was larger than that at the PbO<sub>2</sub> anode in the presence of ultrasound, confirming that ultrasound was more beneficial to indirect electrochemical oxidation mediated by free hydroxyl radicals than by absorbed hydroxyl radicals. The higher gradient of the linear slope fitted to the data obtained in the presence of ultrasound at both BDD and PbO<sub>2</sub> anodes indicates the considerable gain to be made by using ultrasound.

## Acknowledgments

This research was funded by National Natural Science Foundation of China under grant No. 20877001.

## Literature cited

- (1) Cañizares, P.; Lobato, J.; Paz, R.; Rodrigo, M. A.; Sáez, C. Electrochemical oxidation of phenolic wastes with boron-doped diamond anodes. *Water Res.* **2005**, *39*, 2687-2703.
- (2) Morão, A.; Lopes, A.; de Amorim, M. T. P.; Gonçalves, I. C. Degradation of mixtures of phenols using boron doped diamond electrodes for wastewater treatment. *Electrochim. Acta* **2004**, *49*, 1587-1595.
- (3) Zhu, X. P.; Shi, S. Y.; Wei, J. J.; Lv, F. X.; Zhao, H. Z.; Kong, J. T.; He, Q.; Ni, J. R. Electrochemical oxidation characteristics of *p*-substituted phenols using a boron-doped diamond electrode. *Environ. Sci. Technol.* **2007**, *41*, 6541-6546.
- (4) Jüttner, K.; Galla, U.; Schmieder, H. Electrochemical approaches to environmental problems in the process industry. *Electrochim. Acta* **2000**, *45*, 2575-2594.
- (5) Torres, R. A.; Torres, W.; Peringer, P.; Pulgarin, C. Electrochemical degradation of *p*-substituted phenols of industrial interest on Pt electrodes. Attempt of a structure-reactivity

relationship assessment. *Chemosphere* **2003**, 50, 97-104.

(6) Fóti, G.; Gandini, D.; Comninellis, C.; Perret, A.; Haenni, W. Oxidation of organics by intermediates of water discharge on IrO<sub>2</sub> and synthetic diamond anodes. *Electrochem. Solid-State Lett.* **1999**, 2, 228-230.

(7) Feng, Y. J.; Li, X. Y. Electro-catalytic oxidation of phenol on several metal-oxide electrodes in aqueous solution. *Water Res.* **2003**, 37, 2399-2407.

(8) Comninellis, C. Electrocatalysis in the electrochemical conversion/combustion of organic pollutants for waste-water treatment. *Electrochim. Acta* **1994**, 39, 1857-1962.

(9) Panizza, M.; Cerisola, G. Influence of anode material on the electrochemical oxidation of 2-naphthol - Part 1. Cyclic voltammetry and potential step experiments. *Electrochim. Acta* **2003**, 48, 3491-3497.

(10) Panizza, M.; Cerisola, G. Influence of anode material on the electrochemical oxidation of 2-naphthol. Part 2. Bulk electrolysis experiments. *Electrochim. Acta* **2004**, 49, 3221-3226.

(11) Chen, X. M.; Gao, F. R.; Chen, G. H. Comparison of Ti/BDD and Ti/SnO<sub>2</sub>-Sb<sub>2</sub>O<sub>5</sub> electrodes for pollutant oxidation. *J. Appl. Electrochem.* **2005**, 35, 185-191.

(12) Martínez-Huitle, C. A.; Quiroz, M. A.; Comninellis, C.; Ferro, S.; De Battisti, A. Electrochemical incineration of chloranilic acid using Ti/IrO<sub>2</sub>, Pb/PbO<sub>2</sub> and Si/BDD electrodes. *Electrochim. Acta* **2004**, 50, 949-956.

(13) Li, X. Y.; Cui, Y. H.; Feng, Y. J.; Xie, Z. M.; Gu, J. D. Reaction pathways and mechanisms of the electrochemical degradation of phenol on different electrodes. *Water Res.* **2005**, 39, 1972-1981.

(14) Panizza, M.; Cerisola, G. Application of diamond electrodes to electrochemical processes. *Electrochim. Acta* **2005**, 51, 191-199.

(15) Zhu, X. P.; Tong, M. P.; Shi, S. Y.; Zhao, H. Z.; Ni, J. R. Essential explanation of the strong

mineralization performance of boron-doped diamond electrodes. *Environ. Sci. Technol.* **2008**, *42*, 4914 - 4920.

(16) Polcaro, A. M.; Mascia, M.; Palmas, S.; Vacca, A. Electrochemical degradation of diuron and dichloroaniline at BDD electrode. *Electrochim. Acta* **2004**, *49*, 649-656.

(17) Polcaro, A. M.; Vacca, A.; Mascia, M.; Palmas, S. Oxidation at boron doped diamond electrodes: an effective method to mineralise triazines. *Electrochim. Acta* **2005**, *50*, 1841-1847.

(18) Faïd, F.; Contamine, F.; Wilhelm, A. M.; Delmas, H. Comparison of ultrasound effects in different reactors at 20 kHz. *Ultrason. Sonochem.* **1998**, *5*, 119-124.

(19) Del Campo, F. J.; Coles, B. A.; Marken, F.; Compton, R. G.; Cordemans, E. High-frequency sonoelectrochemical processes: mass transport, thermal and surface effects induced by cavitation in a 500 kHz reactor. *Ultrason. Sonochem.* **1999**, *6*, 189-197.

(20) Oliveira, R. T. S.; Garbellini, G. S.; Salazar-Banda, G. R.; Avaca, L. A. The use of ultrasound for the analytical determination of nitrite on diamond electrodes by square wave voltammetry. *Anal. Lett.* **2007**, *40*, 2673-2682.

(21) Saterlay, A. J.; Wilkins, S. J.; Goeting, C. H.; Foord, J. S.; Compton, R. G.; Marken, F. Sonoelectrochemistry at highly boron-doped diamond electrodes: silver oxide deposition and electrocatalysis in the presence of ultrasound. *J. Solid State Electrochem.* **2000**, *4*, 383-389.

(22) Trabelsi, F.; Aït-Lyazidi, H.; Ratsimba, B.; Wilhelm, A. M.; Delmas, H.; Fabre, P. L.; Berlan, J. Oxidation of phenol in wastewater by sonoelectrochemistry. *Chem. Eng. Sci.* **1996**, *51*, 1857-1865.

(23) Leite, R. H. D.; Cognet, P.; Wilhelm, A. M.; Delmas, H. Anodic oxidation of 2,4-dihydroxybenzoic acid for wastewater treatment: study of ultrasound activation. *Chem. Eng. Sci.* **2002**, *57*, 767-778.

- (24) Zhao, G. H.; Shen, S. H.; Li, M. F.; Wu, M. F.; Cao, T. C.; Li, D. M. The mechanism and kinetics of ultrasound-enhanced electrochemical oxidation of phenol on boron-doped diamond and Pt electrodes. *Chemosphere* **2008**, *73*, 1407-1413.
- (25) Trabelsi, F.; Aitlyazidi, H.; Berlan, J.; Fabre, P. L.; Delmas, H.; Wilhelm, A. M. Electrochemical determination of the active zones in a high-frequency ultrasonic reactor. *Ultrason. Sonochem.* **1996**, *3*, S125-S130.
- (26) Panizza, M.; Michaud, P. A.; Cerisola, G.; Comninellis, C. Anodic oxidation of 2-naphthol at boron-doped diamond electrodes. *J. Electroanal. Chem.* **2001**, *507*, 206-214.
- (27) Iniesta, J.; Michaud, P. A.; Panizza, M.; Cerisola, G.; Aldaz, A.; Comninellis, C. Electrochemical oxidation of phenol at boron-doped diamond electrode. *Electrochim. Acta* **2001**, *46*, 3573-3578.
- (28) Cañizares, P.; Sáez, C.; Lobato, J.; Rodrigo, M. A. Electrochemical treatment of 4-nitrophenol-containing aqueous wastes using boron-doped diamond anodes. *Ind. Eng. Chem. Res.* **2004**, *43*, 1944-1951.
- (29) Liu, Y.; Liu, H. L.; Li, Y. Comparative study of the electrocatalytic oxidation and mechanism of nitrophenols at Bi-doped lead dioxide anodes. *Appl. Catal. B: Environ.* **2008**, *84*, 297-302.
- (30) Gherardini, L.; Michaud, P. A.; Panizza, M.; Comninellis, C.; Vatisstas, N. Electrochemical oxidation of 4-chlorophenol for wastewater treatment - Definition of normalized current efficiency ( $\Phi$ ). *J. Electrochem. Soc.* **2001**, *148*, D78-D82.



**Table 1** – Rate constants of *p*-substituted phenols and COD removal at the BDD and PbO<sub>2</sub> anodes in the absence ( $k_{\text{elec}}$ ) and presence ( $k_{\text{sonel}}$ ) of ultrasound (in h<sup>-1</sup>).

Phenols	BDD Anode				PbO <sub>2</sub> Anode			
	Phenols Removal		COD Removal		Phenols Removal		COD Removal	
	$k_{\text{elec}}$	$k_{\text{sonel}}$	$k_{\text{elec}}$	$k_{\text{sonel}}$	$k_{\text{elec}}$	$k_{\text{sonel}}$	$k_{\text{elec}}$	$k_{\text{sonel}}$
<i>p</i> -NO <sub>2</sub>	0.4635	1.9004	0.1747	0.4241	0.5349	1.6522	0.1261	0.1719
<i>p</i> -CHO	0.2759	1.1538	0.1256	0.4311	0.1966	0.4451	0.0579	0.1000
<i>p</i> -H	0.2051	1.2148	0.1544	0.3943	0.2503	0.7246	0.0455	0.0487
<i>p</i> -CH <sub>3</sub>	0.1491	0.7846	0.1195	0.3270	0.1140	0.2590	0.0221	0.0252
<i>p</i> -OCH <sub>3</sub>	0.1933	0.7104	0.1270	0.3966	0.2046	0.9259	0.0239	0.0249

**Figure captions:**

**FIGURE 1.** Evolution of (A) substrate concentration, and (B) COD at the BDD anode; and (C) substrate concentration, and (D) COD at the PbO<sub>2</sub> anode, during bulk electrolysis in the absence (solid symbols) and presence (open symbols) of ultrasound. Symbols: (■) *p*-nitrophenol, (●) *p*-hydroxybenzaldehyde, (▲) phenol, (▼) *p*-cresol, and (★) *p*-methoxyphenol.

**FIGURE 2.** %Synergy for the five *p*-substituted phenols with regard to (A) phenol degradation, and (B) COD degradation at the BDD anode, and for (C) phenol degradation, and (D) COD removal at the PbO<sub>2</sub> anode.

**FIGURE 3.** Cyclic voltammograms of the *p*-substituted phenols at the BDD and PbO<sub>2</sub> electrodes in the absence and presence of ultrasound: (A) *p*-nitrophenol, (B) *p*-hydroxybenzaldehyde, (C) phenol, (D) *p*-cresol, and (E) *p*-methoxyphenol at the BDD electrode; (F) *p*-nitrophenol, (G) *p*-hydroxybenzaldehyde, (H) phenol, (I) *p*-cresol, and (J) *p*-methoxyphenol at the PbO<sub>2</sub> electrode. Symbols: (0) blank, (1) first cycle and (2) second cycle in the absence of ultrasound, (1') first cycle and (2') second cycle in the presence of ultrasound.

**FIGURE 4.** Time evolution of electrogenerated oxidant concentration at the BDD anode in the absence (■) and presence (□) of ultrasound.

**FIGURE 5.** Time evolution of hydroxyl radical concentration at BDD (A) and PbO<sub>2</sub> (B) anodes in the absence (■) and presence (□) of ultrasound.

**FIGURE 6.** Relationships (A) between rate constant (*k*) of *p*-substituted phenols and Hammett's constant ( $\sigma$ ) at the BDD electrode, and (B) between rate constant (*k*) of *p*-substituted phenols and the initial surface concentration ( $\Gamma$ ) at the PbO<sub>2</sub> anode, in the absence (●) and presence (○) of ultrasound.

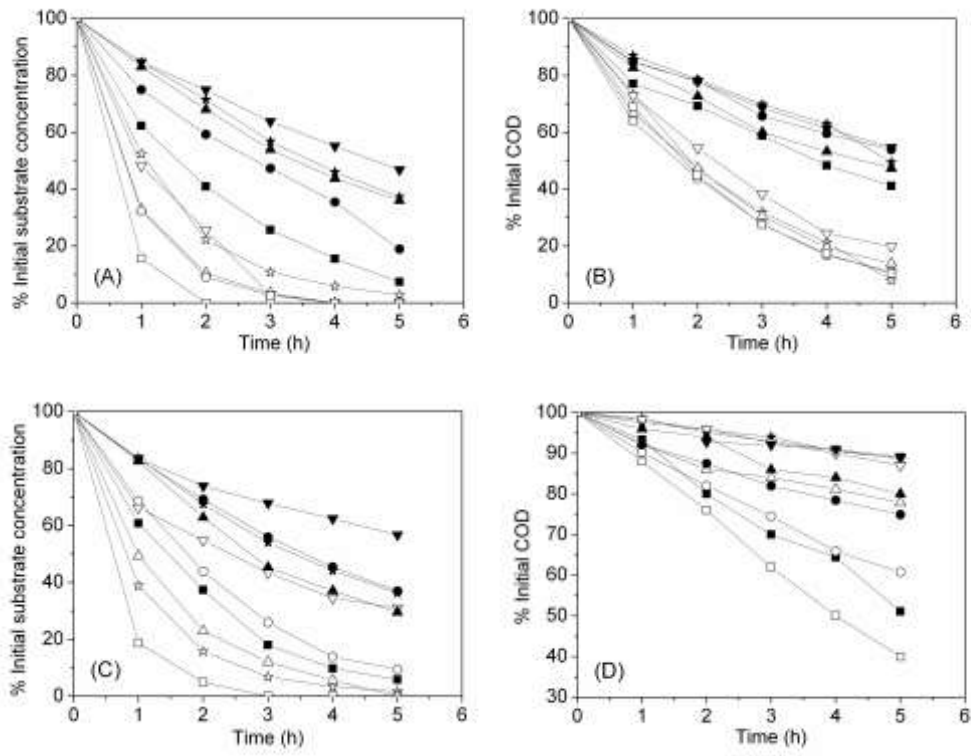


Figure 1

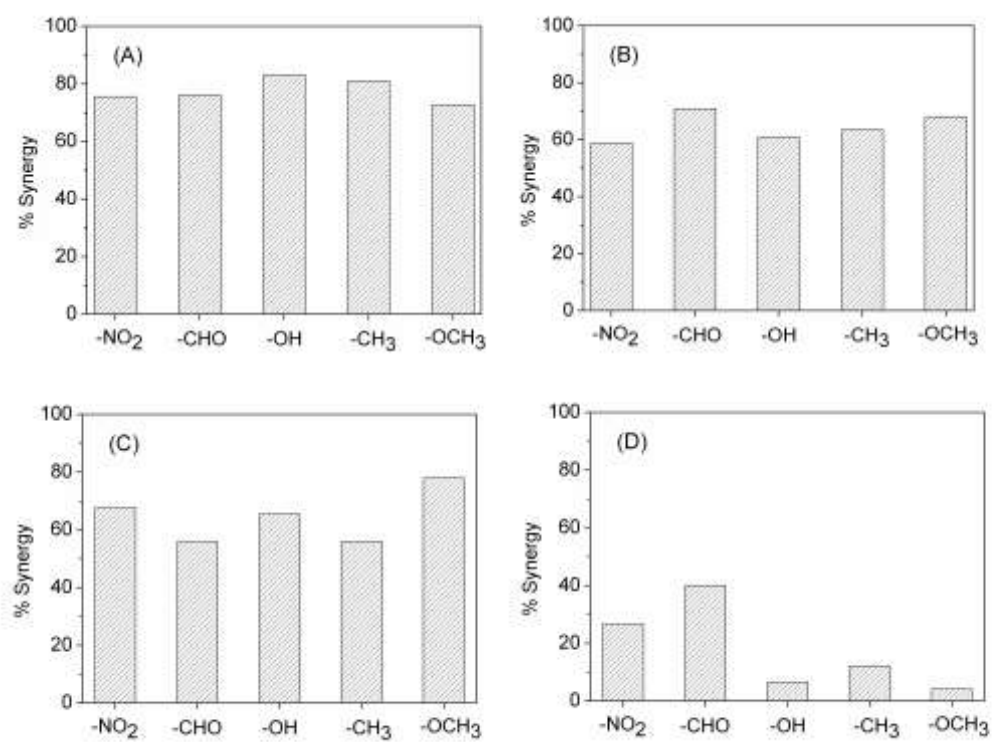


Figure 2

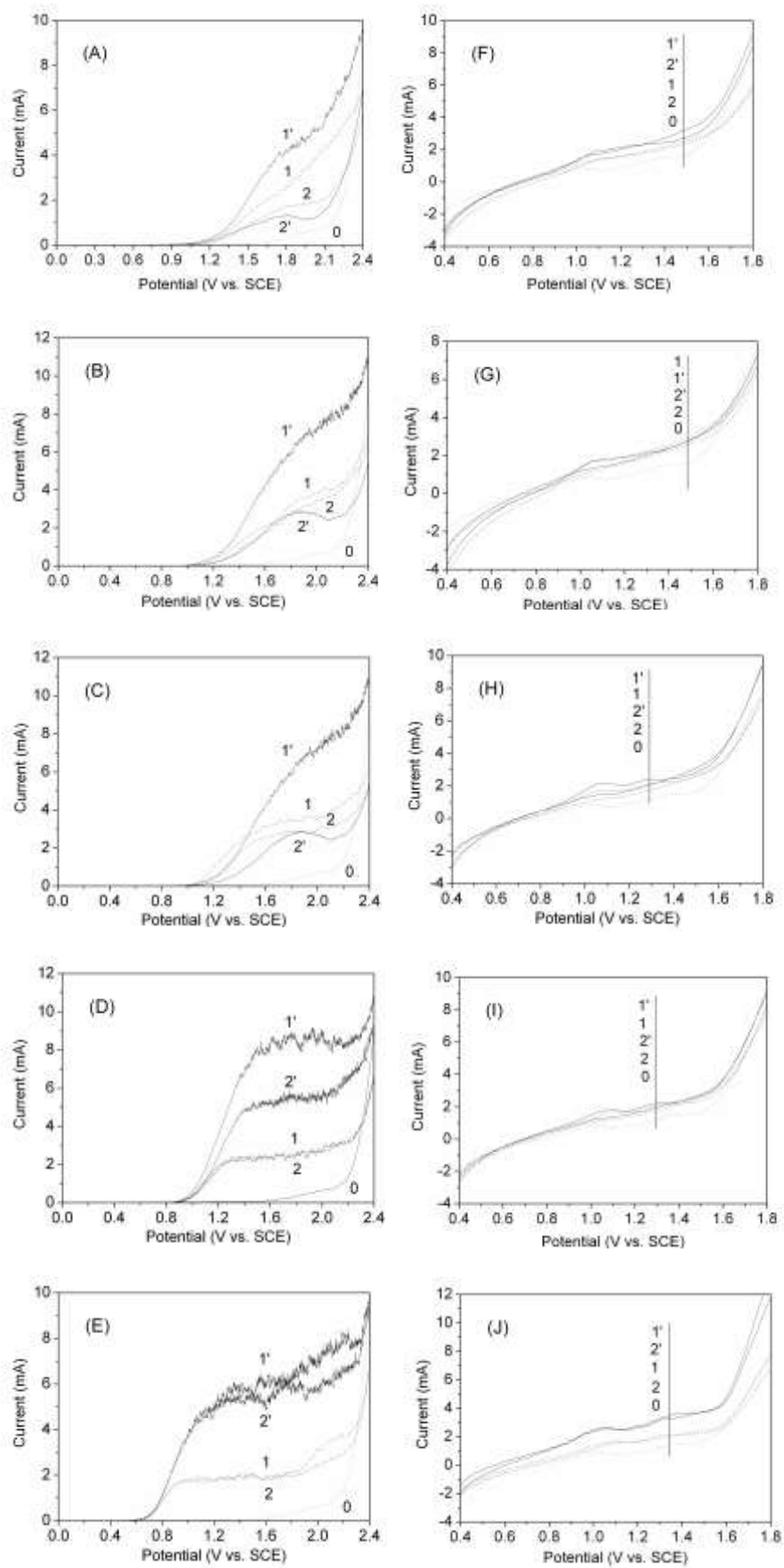


Figure 3

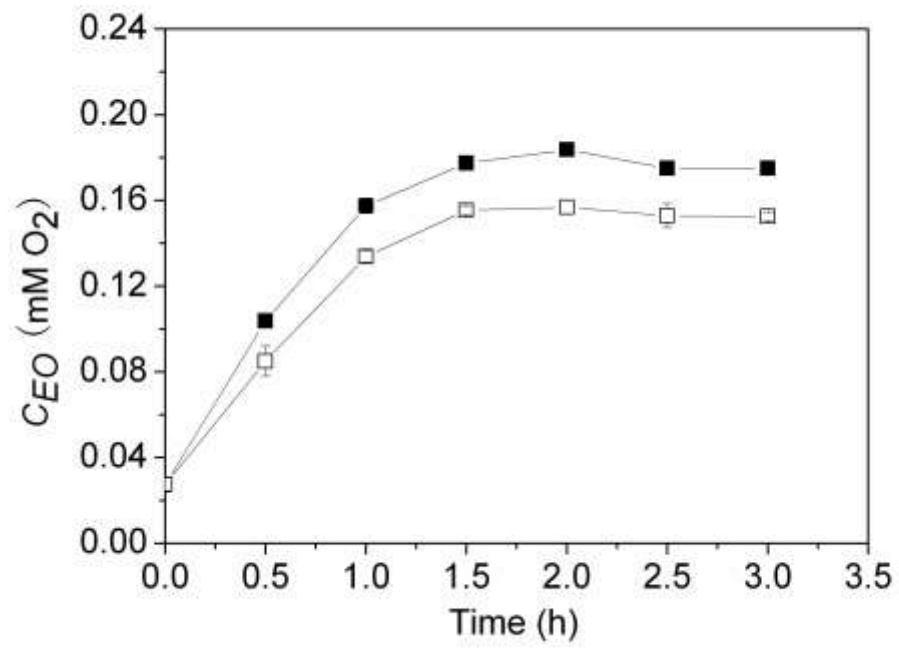
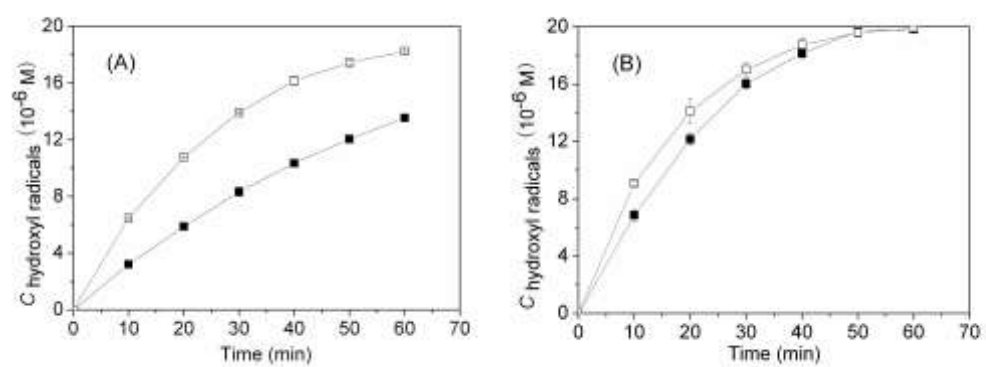
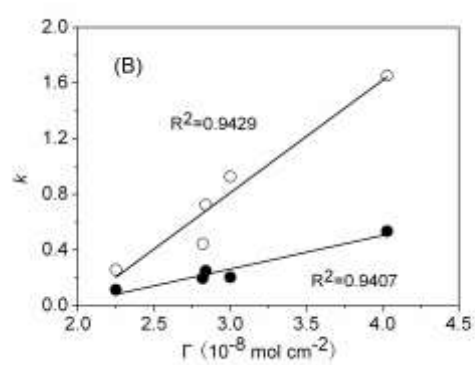
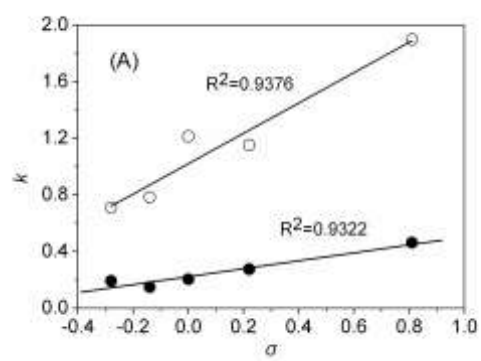


Figure 4



**Figure 5**



1

2 **Figure 6**